Journal of Theoretical Biology 539 (2022) 111062

Contents lists available at ScienceDirect

Journal of Theoretical Biology

journal homepage: www.elsevier.com/locate/yjtbi

A simple one-dimensional map-based model of spiking neurons with wide ranges of firing rates and complexities

Alireza Bahramian [a], Janarthanan Ramadoss [b], Fahimeh Nazarimehr [a], Karthikeyan Rajagopal [c], Sajad Jafari [a,d], Iqtadar Hussain [e,*]

[a] Department of Biomedical Engineering, Amirkabir University of Technology (Tehran Polytechnic), Iran
[b] Centre for Artificial Intelligence, Chennai Institute of Technology, India
[c] Centre for Nonlinear Systems, Chennai Institute of Technology, Chennai, India
[d] Health Technology Research Institute, Amirkabir University of Technology (Tehran Polytechnic), Iran
[e] Mathematics Program, Department of Mathematics, Statistics and Physics, College of Arts and Sciences, Qatar University, 2713 Doha, Qatar

ARTICLE INFO

Article history:
Received 29 July 2021
Revised 1 February 2022
Accepted 8 February 2022
Available online 12 February 2022

Keywords:
Neuron model
Map
Spike
Firing rate
Complexity

ABSTRACT

This paper introduces a simple 1-dimensional map-based model of spiking neurons. During the past decades, dynamical models of neurons have been used to investigate the biology of human nervous systems. The models simulate experimental records of neurons' voltages using difference or differential equations. Difference neuronal models have some advantages besides the differential ones. They are usually simpler, and considering the cost of needed computations, they are more efficient. In this paper, a simple 1-dimensional map-based model of spiking neurons is introduced. Sample entropy is applied to analyze the complexity of the model's dynamics. The model can generate a wide range of time series with different firing rates and different levels of complexities. Besides, using some tools like bifurcation diagrams and cobwebs, the introduced model is analyzed.

1. Introduction

Scientists use computational models to achieve a better insight into biological complex systems (Ma and Tang, 2017; Wu et al., 2019; Baer et al., 2021). There is a famous quote from Einstein that everything should be made as simple as possible, but no simpler (Sanchez, 2006). This quote can be considered in the line of holism theory. It can be helpful to approach biological phenomena computationally (Ma and Tang, 2015). In this way, it is needed to neglect lots of details about neurons as biological phenomena to pay attention to the principles of the main dynamics (Girardi-Schappo et al., 2013; Ma et al., 2019). Mathematical models of neurons are used to study the behaviors of neuronal populations (Wang and Ma, 2018; Rouhani et al., 2021). The basis of these mathematical models is dynamical equations of single neurons (Khaleghi et al., 2019). Various models have been developed to represent a single neuron's behaviors (Herz et al., 2006; Bhalla and Le Novère, 2012). One of the first approaches to model neurons' behaviors is based on the cable/circuits theories (Liu et al., 2019). These models try to regenerate neurons' responses and dynamics by paying attention to their structures and topologies (Mainen and Sejnowski, 1996). These models were not suitable for studying collective behaviors of neurons in a network since they needed many computational operations (Bush and Sejnowski, 1993). To tackle this problem, several models are introduced to ignore some unnecessary details and reduce the number of equations (Brette and Pillow, 2015). These models focus on the influence of the different ions' currents on spikes and sub-threshold states (Rotstein et al., 2006; Ge et al., 2018). Hodgkin and Huxley have suggested a conductance-based model capable of regenerating lots of neurons' behaviors like periodic, chaotic bursts and spikes (Hodgkin and Huxley, 1990). The model was a 4-dimensional ordinary differential equation (ODE) (Hodgkin and Huxley, 1990). More simplified versions of the Hodgkin Huxley (HH) model were used to decrease computational complexity (B. A. y. Arcas, A. L. Fairhall, and W. Bialek, , 2003; Doya and Selverston, 1994). For instance, a 2-dimensional version of HH was used to model the muscle fibers (Morris and Lecar, 1981). FitzHugh Nagumo was another 2-dimensional ODE model of neurons. It considers the permeability of ions' passing instead of ion channels' conductance (Nagumo et al., 1962; FitzHugh, 1955). Another model was developed by Wilson that was tuned based on experimental data of ion currents (Wilson and Cowan, 1972). The 3-dimensional Hindmarsh Rose model was developed based on the membrane's fast and slow currents. In the 2-dimensional model

* Corresponding author.
E-mail address: Iqtadarqau@qu.edu.qa (I. Hussain).

https://doi.org/10.1016/j.jtbi.2022.111062
0022-5193/

of Izhikevich, a resetting mechanism has been considered that makes the 2-dimensional model capable of reproducing more complex behaviors (Izhikevich, 2004). Besides, inspired by HH, some other models have been designed based on the phase space analyses (Izhikevich, 2004; FitzHugh, 1961). A piecewise model of neurons has been introduced to investigate the mechanism of tabu learning neurons (Bao et al., 2020). The interaction of the neurons and their synaptic activities is a matter of interest for researchers to design proper computational frameworks (Bao et al., 2020). Moreover, some models have been developed to investigate the magnetic inductions among neurons (Bao et al., 2020). For instance, the effect of external magnetic flux on chaotic/hyperchaotic neurons has been investigated by modifying the Hindmarsh Rose model (Wang et al., 2020). Besides, memristor based models of neurons have been developed. They are popular because of their capacity to show magnetic interaction among neurons (Bao et al., 2020; Zhang et al., 2020). For instance, a fractional order type of memristor based model for neurons has been used to investigate collective behaviors of neurons (He, 2020). In addition, there are some simpler models like integrated and fire models, which are not capable of generating bursts. However, because of their simplicity, they have gotten a large amount of attention (Badel et al., 2008). A light-driven neuron model was studied in (Gentili et al., 2021). A new version of the fractional leaky integrate-and-fire model was investigated in (AbdelAty et al., 2022). A Chua corsage memristor-based neuron model and its dynamics were discussed in (Dong et al., 2021).

Besides ODE models, map-based models have grabbed lots of attention themselves (Girardi-Schappo et al., 2013). Although these models are simpler, they can generate complex neural behaviors (Ibarz et al., 2011). These models are compatible with the principles of the holistic theory while they focus on the overall functions of neurons (Khaleghi et al., 2019). The equations of map-based models are usually more elegant than ODE-based neural models (Maslennikov and Nekorkin, 2014). In these models, details are ignored as much as possible (Rulkov et al., 2004). Therefore, their computational costs are much lower (Ibarz et al., 2011). For instance, in the 1-dimensional map-based models, the membrane's voltage is the only variable (Pasemann, 1997). Various map-based models have been introduced (Ibarz et al., 2011). Some of them are based on the discretization of ODE models. For example, the Izhikevich map-based model was developed using the discretization of the Izhikevich by the Euler method (Izhikevich, 2003). Other models like the 2-dimension Rulkov model were designed based on the fast and slow neuronal dynamic (Rulkov, 2002). Some map-based models have been analyzed using phase space and cobweb (Channell et al., 2007; Ibarz et al., 2008; Courbage and Nekorkin, 2010). Piecewise map-based models of neurons usually were designed in this way (Izhikevich and Hoppensteadt, 2004; LoFaro and Kopell, 1999). These piecewise models were capable of being coupled in different modes (Cazelles et al., 2001). A 1-dimensional map based on the logistic map was designed that shows a large variety of neuronal behaviors (Mesbah et al., 2014). A 1-dimension map-based model with important parameters has been designed in (Medvedev, 2005). The memristor-based implication of the Rulkov model, which is a discrete map, has also been proposed to investigate the magnetic induction effects on the neurons' behaviors (Li et al., 2022).

The firing rate of spiking neurons is one of the crucial features of neural signals (Obeid and Wolf, 2004). To encode the function of the brain, researchers pay lots of attention to this feature (Rolls and Treves, 2011; Gibson et al., 2012). Considering its importance, different models have been developed to generate spikes with wide ranges of firing rates (Schwalger and Chizhov, 2019; Pietras et al., 2020). Besides, the complexity of neuronal systems has always been a matter of interest for neuroscientists (Guo et al., 2020; Churchland and Shenoy, 2007). Sample entropy is a valuable measure of the complexity of the neuronal signals (Zhang et al., 2009; Jia et al., 2017).

In this paper, a new map-based model with a simpler equation than most previous neuronal models is introduced. The dynamics of the model are investigated using cobweb plots and analytical tools in section 2. The model's capability to generate wide ranges of firing rates, inter-spike interval (ISI), and complexities is demonstrated in section 3. The conclusion of the paper is presented in section 4.

2. The proposed model

To design a map that mimics the behavior of spiking neurons, a neuronal spiking signal is considered as Fig. 1 (A). The figure is an extracellular recorded signal of a neuron (Palmieri et al., 2015; Henze et al., 2000). Voltage fluctuations can be seen when the neuron is in its rest state. The sources of these fluctuations can be external noise and the dynamics of neuron ion channels (Bahramian et al., 2019; Kasimova et al., 2018; Destexhe et al., 2001). In this paper, a map with the potential of representing these fluctuations is designed. Fig. 1 (B) demonstrates action potential simulated with a Hodgkin-Huxley model (Naundorf et al., 2006). This action potential can be considered as a single spike. In this figure, the points A, B, and C are in the rest state. Point D shows the peak of the spike. Points E and F again are located in the rest state. Considering Fig. 1 (C), if a map (with values between 0 and 1) tries to regenerate the time series of Fig. 1 (B), its phase space and the cobweb should be like Fig. 1 (C). Points A, B, C, and F should be in the blue square named the rest state region. When a spike happens, point D, as the peak of the spike is located in the green region (spike region). Point E in the assumed phase space is located in the red region.

In this paper, a piecewise map is designed with two pieces. The first piece represents the rest state (blue region in Fig. 1 (C)). The second piece is supposed to empower the map to spike (green region) and then reset the map time series to the rest state (red region). The 1-dimensional equation of the proposed spiking neuron is shown in Eq. (1).

$$x(i+1) = a + bx(i) module(1) \tag{1}$$

Where x is considered as the voltage of a neuron.a and b are the model parameters. The module (1) of the right side of the equation is calculated, and its result is considered the value of $x(i+1)$. The equation is piecewise since it uses the module (1) function. Instead of writing two different equations for each piece, in this work, module (1) is used for breaking $(a+bx)$ into two separated parts. The map is designed in the interval [0, 1], and the initial value is considered in it. So x values change just in that interval. Applying module (1) allows consideration of a lower number of equations for the introduced piecewise map. In all simulations of this paper, parameters are considered $a \in [0.15, 0.25]$ and $b \in [-1.15, -1]$. The model has two equilibrium points in the studied interval of parameters (the yellow points in Fig. 2). The values of the equilibrium points can be calculated as follows:

if $0 < (a + bx(i)) < 1 \rightarrow module((a + bx(i)), 1) = (a + bx(i)) \rightarrow$

$$E(1) = \frac{a}{1-b}$$

if $(a + bx(i)) < 0 \rightarrow module((a + bx(i)), 1) = (a + bx(i) + 1) \rightarrow$

$$x(i) = a + bx(i) + 1, \rightarrow x(i) = \frac{a+1}{1-b}, \rightarrow E(2) = \frac{a+1}{1-b} \tag{2}$$

Therefore, an equilibrium point exists in each of the two pieces. The types of these equilibrium points are determined considering the results of Eq. (3):

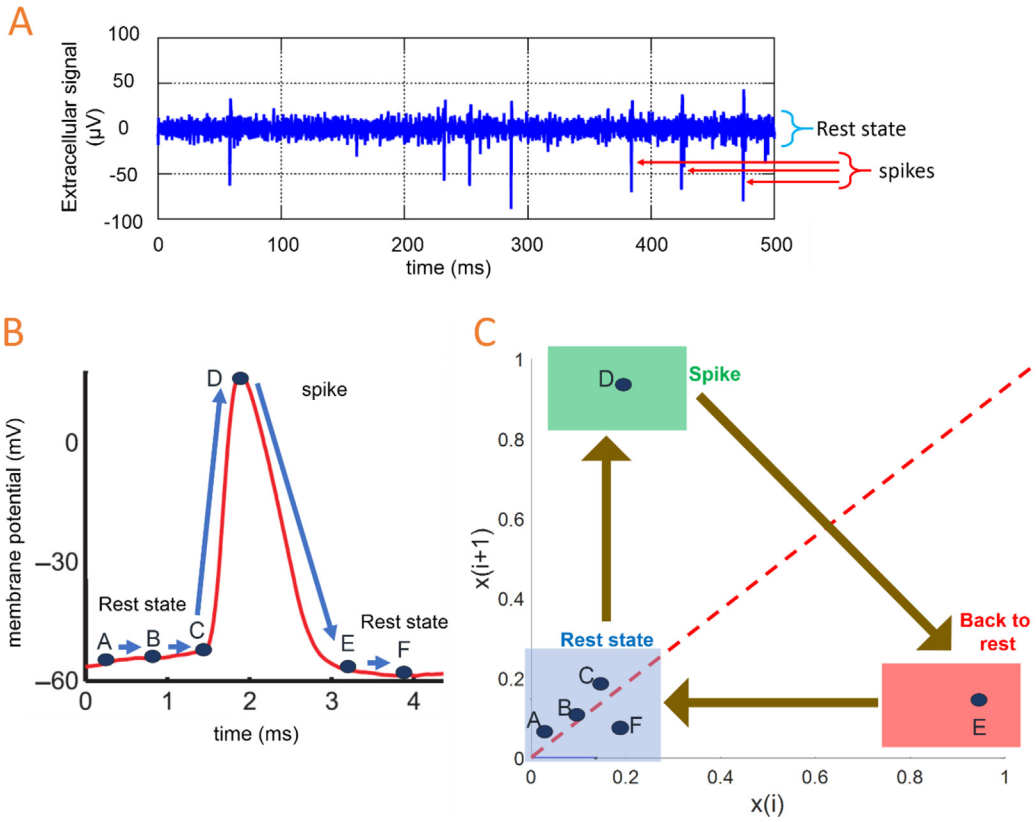

Fig. 1. Inspiration from spiking time series to design map-based model of a spiking neuron. A) time-series of a neuron's membrane voltage (extracellular) (Palmieri et al., 2015; Henze et al., 2000). Before and after spikes, when the neuron is in the rest state, fluctuations in the voltage can be seen. B) Action potential simulated with the Hodgkin-Huxley model (Naundorf et al., 2006). The points A, B, C, D, E, and F are considered to explain the main dynamic of a spike and get inspiration to design a map that can model spikes. C) Inspired from the spike time series, in phase space, the blue region of the map represents the rest state, the green part represents spike, and the red part sends back the cobweb trajectory to the rest state.

for the first equilibrium point $(E\ (1))\left(\frac{a}{1-b}\right)$:

$$y = a + bx \rightarrow \dot{y} = b \overset{|b|>1}{\rightarrow} E(1)\ \textit{is unstable}$$

for the second equilibrium point $(E(2))\left(\frac{a+1}{1-b}\right)$:

$$y = a + bx + 1 \rightarrow \dot{y} = b \overset{|b|>1}{\rightarrow} E(2)\ \textit{is unstable} \tag{3}$$

So, the system has two unstable equilibrium points in the studied parameters. The map plot is shown in Fig. 2 (A) with black lines when the identity line is plotted with a red line ($a = 0.15$ and $b = -1.1$). The cobweb of the system is demonstrated in Fig. 2 (B). The module (1) function breaks the linear equation into two pieces. The piece in the neighborhood of E (1) is responsible for generating the rest state fluctuations of the voltage. The unstable E (1) gradually moves the trajectory away from it (Fig. 2 (C)). Finally, the trajectory jumps to the other piece, and this jump is considered as a spike (Fig. 2 (C), (D)). The piece in the neighborhood of E (2) causes the trajectory to be placed in the neighborhood of E (1) again, after its jump (spike) (Fig. 2 (B), (D)). Fig. 2 (D) shows how these two pieces represent the rest state region, spike region, and resetting (back to rest) regions.

3. The studied measures

Here three measures are used to study the dynamics of the neuronal model. These measures are discussed in the following.

A sample of the map's time series is demonstrated in Fig. 3 for $a = 0.15$ and $b = -1.1$. The threshold value of 0.4 is selected to calculate the firing rate of spikes. Therefore, when a point of time series has a value larger than 0.4, it is considered a spike.

The firing rate of spikes is calculated as:

$$\textit{firing rate} = \frac{\textit{the number of spike points}}{\textit{the number of all points}} \tag{4}$$

The spike points are the ones with values larger than 0.4. The number of all the time series' points is set at 1000.

Besides the firing rate of spikes, the sample entropy of the time series is calculated. The sample entropy is an index of complexity. It calculates how many samples of a time series (for instance , t number) are needed to predict the following sample $((t+1)th)$.

For a given time series $\{x(i)\}$, $(i = 1, \cdots, N)$, the sample entropy algorithm is calculated as following (Richman and Moorman, 2000):

(1) Reconstruct a group of time series based on the given signal:

$$X_i(m) = \{x_i, x_{i+\tau}, \cdots, x_{i+(m-1)\tau}\}, i = 1, 2, \cdots, N - m + 1 \tag{5}$$

where $X_i \in R^m$, τ, and m are time delay and embedding dimensions, respectively. $\tau = 1$ is set.

(2) For X_i and X_j, the distance is calculated with the following assumptions (for m dimensional embedded state space):

$$r = 0.2 \times (\textit{StandardDeviation})$$

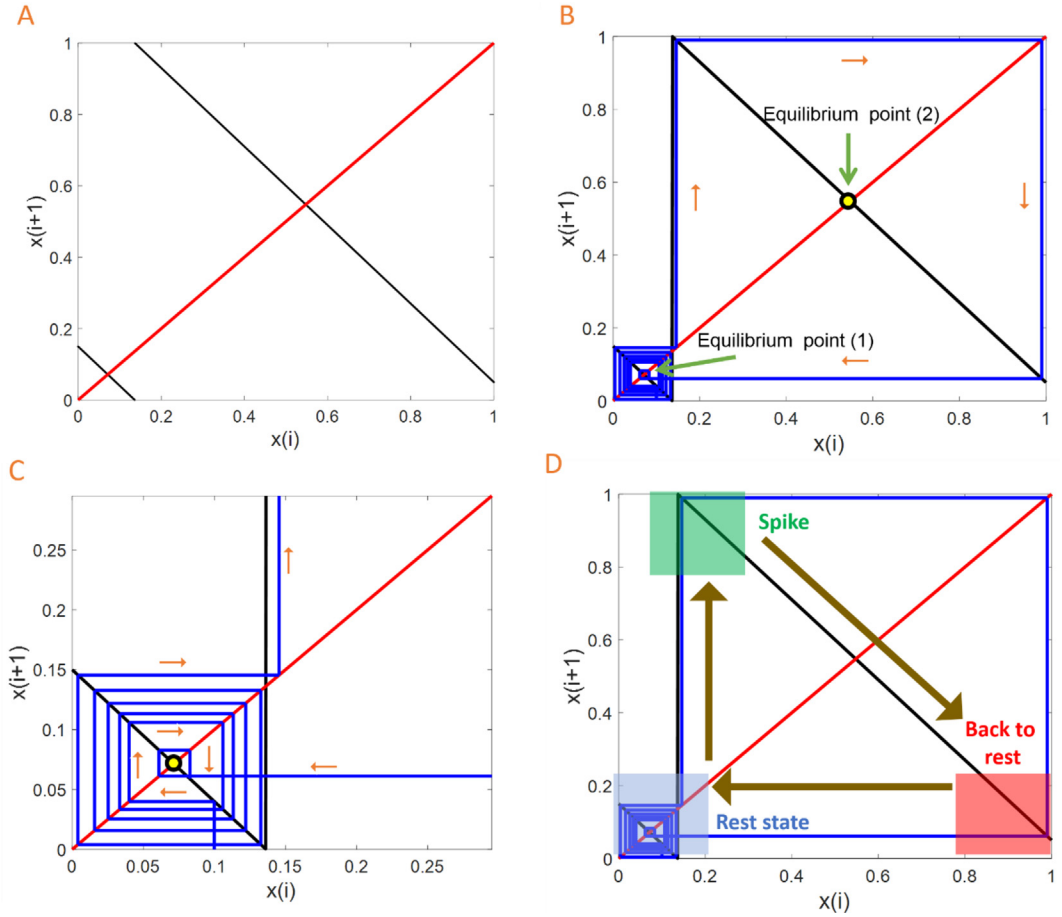

Fig. 2. A) The map plot with black lines when the red line demonstrated the identity line. B) The map has two unstable equilibrium points, which are shown with the yellow dots. The trajectory's directions are shown with arrows. C) The E (1) gradually moves the trajectory away from itself. When the trajectory is in the E (1) neighborhood, it is considered that the neuron is in the rest state. D) the piece in the E (1) neighborhood can represent the rest state (the blue region). The piece in the E (2) neighborhood empowers the map to generate spikes.

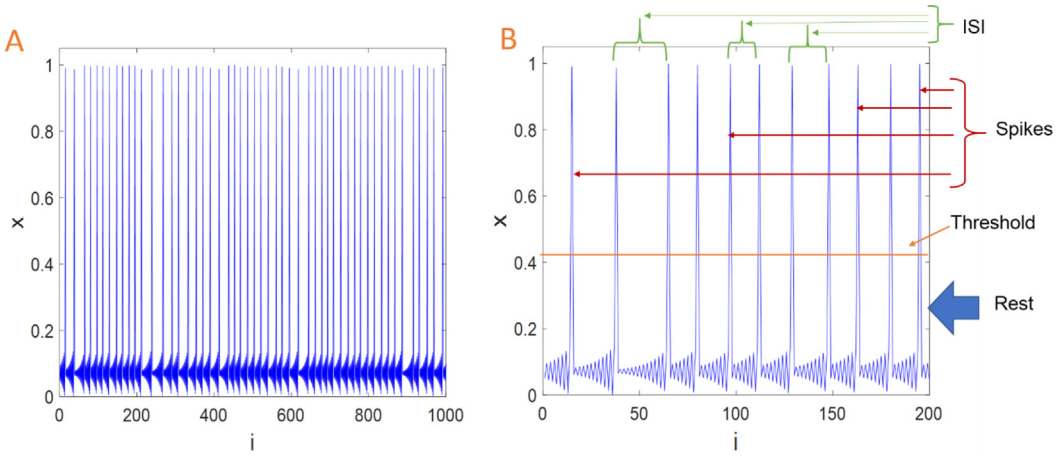

Fig. 3. A sample of the map's time series. A) the values of the dynamical variable (x) in parameters $a = 0.15$ and $b = -1.1$. B) the zoomed version of part (A) for better visualization. The considered threshold that separates spike points from the rest ones is plotted with an orange line. Red arrows show the value of some points which are considered spikes. ISI is the number of samples among every two spikes, and its schematic is drawn with the green arrows.

$$B_i^m(r) = \frac{1}{N-m-1} \sum_{j=1,\ i\neq j}^{N-m} Heaviside(r - X_i = X_j)_\infty \qquad B^m(r) = \frac{1}{N-m} \sum_{j=1}^{N-m} B_i^m(r)$$

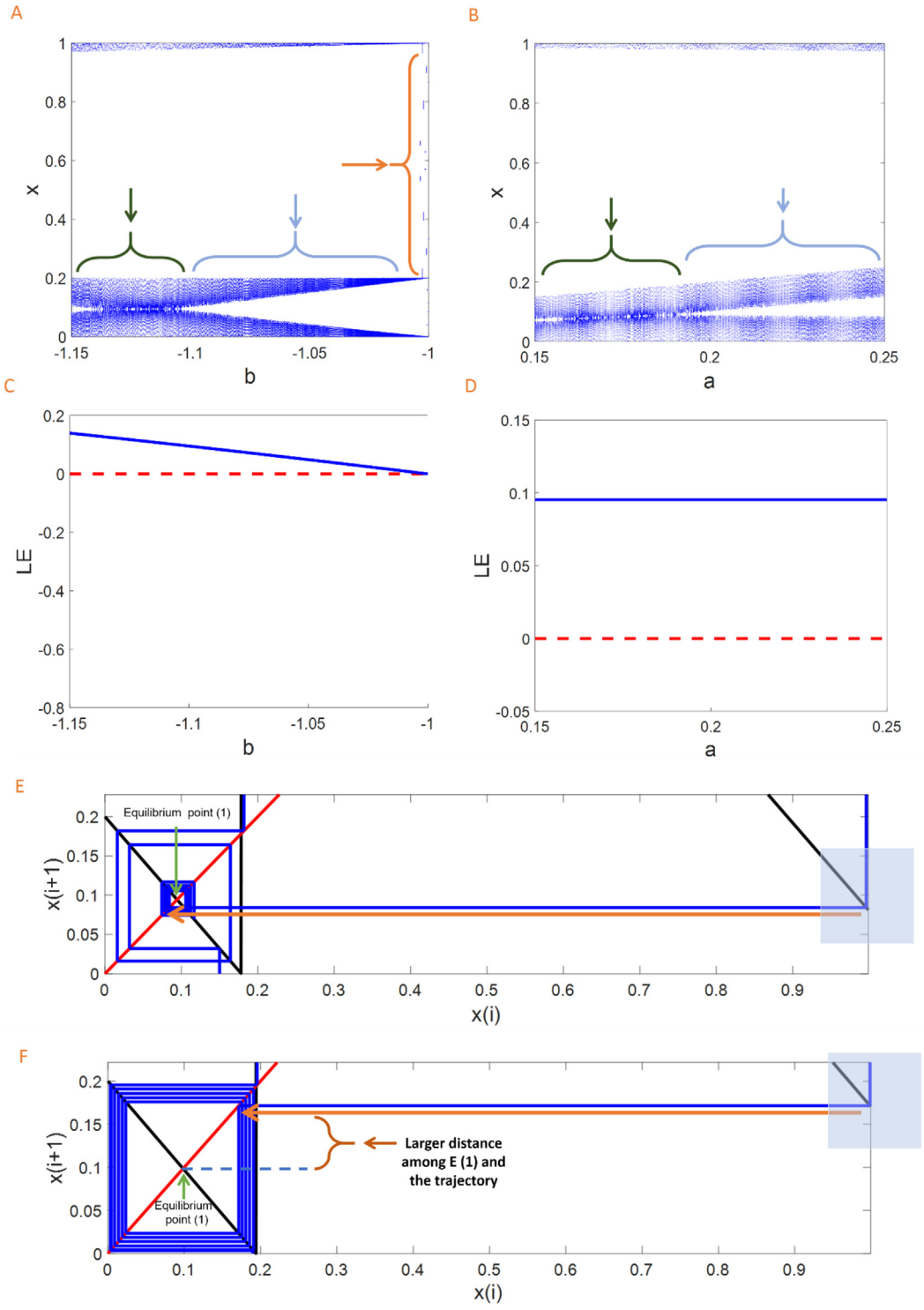

Fig. 4. The bifurcation and cobweb diagrams of the proposed map. A) the bifurcation diagram by changing b and constant $a = 0.2$; B) the system's bifurcation versus a and constant $b = -1.1$; C) Lyapunov exponent by varying b; D) Lyapunov exponent by varying a; E) cobweb diagram for $a = 0.2$ and $b = -1.12$; the trajectory after a spike is reset to a value that is near to E (1). F) cobweb diagram in $a = 0.2$ and $b = -1.03$; the trajectory after a spike is reset to a value that has more distance from E (1) rather than the trajectory in part (E).

$$B(r) = \frac{1}{2}(N-m-1)(N-m)(B^m(r)) \tag{6}$$

where $B(r)$ is the total templates that are matched in m dimension. The same calculations have been done for $m+1$ dimension embedded state space:

$$A_i^m(r) = \frac{1}{N-m-1}\sum_{j=1,\ i\neq j}^{N-m} Heavside(r)(r - X_i = X_j)_\infty$$

$$A^m(r) = \frac{1}{N-m}\sum_{j=1}^{N-m} A_i^m(r)$$

$$A(r) = \frac{1}{2}(N-m-1)(N-m)(A^m(r)) \tag{7}$$

where A (r) is the total templates that are matched in m dimension.

(3) In this paper considering m = 2, sample entropy is calculated with the following formula:

$$\mathrm{SamEn}(m,r,N) = -\log(\frac{A(r)}{B(r)}) \tag{8}$$

The average ISI is also calculated for the time series. First, the number of samples between two spikes is computed, and then their average is presented as the average ISI. Besides, the Lyapunov exponent (Batista et al., 2002) of the introduced pricewise map is calculated.

In the next section, bifurcation diagrams of the system are plotted. Also, the value of sample entropy, the firing rate of spikes, and its average are calculated.

4. Results

Bifurcation diagrams are powerful tools in the study of dynamical systems. The bifurcation diagrams of the proposed map are demonstrated in Fig. 4. In the simulations, the first 1000 samples of the signal are removed as the transient time. The following 1000 samples are considered to plot bifurcation diagrams and calculate measures. For the values of b near to -1, the map is not proper to generate spikes (shown with the orange arrow in Fig. 4 (A)). For these b values, the map slope is low, and the cobweb trajectory is getting away from E (1) very slow. In both parts (A) and (B) of Fig. 4, two bands at the bottom and the top of bifurcation diagrams can be seen. The bottom band has two sub-bands. The top bands show the values of spikes. The bottom bands demonstrate the fluctuations of the trajectories in the rest state (in the neighborhood of E (1)). The bottom band has two sub-bands in Fig, 4 (A). In $b \in [-1.15, -1.1]$, these two bands are so close and merge (shown with green arrow). However, in $b \in [-1.1, -1]$ (shown with the blue arrow), the bottom band in Fig. 4 (A) has two branches. This phenomenon happens because of the resetting mechanism of the map, which is shown in Fig. 4 (E) and (F). In $b \in [-1.1, -1]$, after each spike, the part of the map which is in the piece of E (2), demonstrated with a blue square in Fig. 4 (E) and (F), sends the trajectory to the piece of E (1). When the trajectory is near to E (1), Fig. 4 (E), shown by the orange arrow, it spans almost all values that are in the neighborhood of E (1). When it gradually goes away from a value that is very near to E (1), a fully dotted bottom band in Fig. 4 (A) can be seen ($b \in [-1.15, -1.1]$, shown by green arrow). Increasing the value of b from -1.1 to -1 causes the trajectories to have more distance from E (1) (Fig. 4 (F), shown by the brown arrow). Consequently, for values around the E (1), there is no data in $b \in [-1.1, -1]$ shown in Fig. 4 (A) by the blue arrow. Besides, the bottom band of Fig. 4 (A), for b values in the interval -1.05 and -1, is more solid than the bottom band where b is in the interval $[-1.15, -1.1]$. Fig. 4 (C) demonstrates the Lyapunov exponent of the introduced map-based neural model for various b ([-1.15, −1]). Wolf method is used to calculate Lyapunov exponents of the system with run time 10,000 (Wolf et al., 1985). The Lyapunov exponents for smaller values of b (which has larger absolute values) are larger positive values rather b larger values. Therefore, larger absolute values of b have stronger chaotic dynamics. Fig. 4 (C) shows the Lyapunov exponent of the map by varying parameter a ([0.15, 0.25]). Changing the values of a does not affect the Lyapunov exponent values.

The sample entropy is calculated for different values of parameters a and b (Fig. 5). The map can generate time series with sample entropy values in the interval $[0, 0.3]$. In small b values, increasing the value of $a \in [0.15, 0.25]$ increases the sample entropy. However, the largest value of sample entropy happens when both a and b are very small. The smallest sample entropy values emerge when the value of a and b are around 0.15 and -1.054, respectively. Comparing Fig. 4 (A) with Fig. 5 in $a = 0.2$, the model presents time series with more complexity. The complexity of the time series in $b \in [-1.05, -1]$ where the two sub-bands of the bottom band are wholly separated is more than the situation of $b \in [-1.5, -1.1]$ where the two sub-bands of the bottom band are nearer to each other. Therefore, the time series are more complex for these sets of parameters, and their reset values have longer distances to E (1). On the other hand, the comparison can be made between Fig. 4 (B) where$b$ = −1.12by changing a and Fig. 5. Since b=−1.12, changing the value of a does not change the complexity of the time series very much.

Spike's firing rate is calculated for various parameters, as shown in Fig. 6. The largest values of spike's firing rate emerge where a and b are small. In larger b, increasing the value of a increases the spike's firing rate. On the other hand, for smaller values of b, increasing a decreases the spike firing rate. Comparing Fig. 4 (A) with Fig. 6, in $a = 0.2$, increasing the value of b from -1.15 to -1 causes the spike's firing rate first to decrease and then to increase. In the case of low firing rates, where the trajectory values after each spike are reset near E (1) (like Fig. 4. (E)), the trajectory remains in the rest for more time. Therefore, the number of its spikes decreases for a fixed number of samples.

The average of ISIs for the time series is calculated by changing a and b (Fig. 7). The average of ISIs has smaller values for both larger and smaller values of b. For larger b, increasing the value of a results decreases the average ISI with a very small slope. For large values of b, increasing a increases the average of ISIs. The average ISI has its maximum values, where a has its smallest value, and the value of b is -1.08. Comparing Fig. 6 and Fig. 7, the average ISI and spike's firing rate have an inverse relationship with each other.

In this work, a 1-dimensional map-based neuronal model of spikes was introduced. In models like 1-dimensional modified logistic map (Mesbah et al., 2014) and some other piecewise models of neuronal behaviors (Zandi-Mehran et al., 2020), the voltage

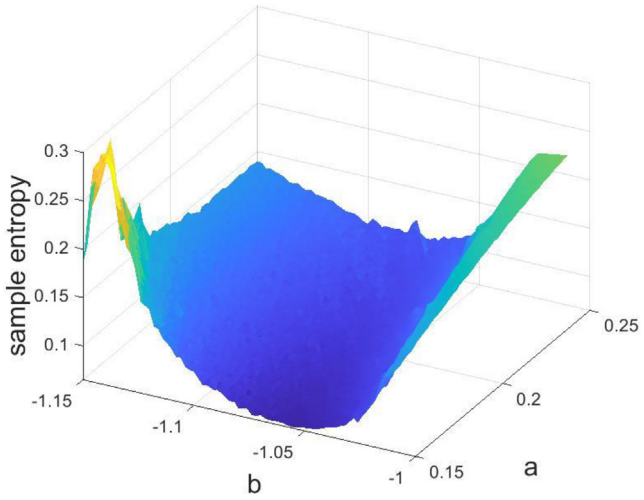

Fig. 5. Sample entropy for different values of a and b. The maximum value of sample entropy is for time series in $a = 0.15$ and $b = -1.15$. Compared to Fig. 4 (A), increasing b values from -1.1 to -1 causes the increase of the generated time series' complexities. Compared to Fig. 4 (B), increasing the value of a in $b = -1.1$ does not change the value of the sample entropy so much.

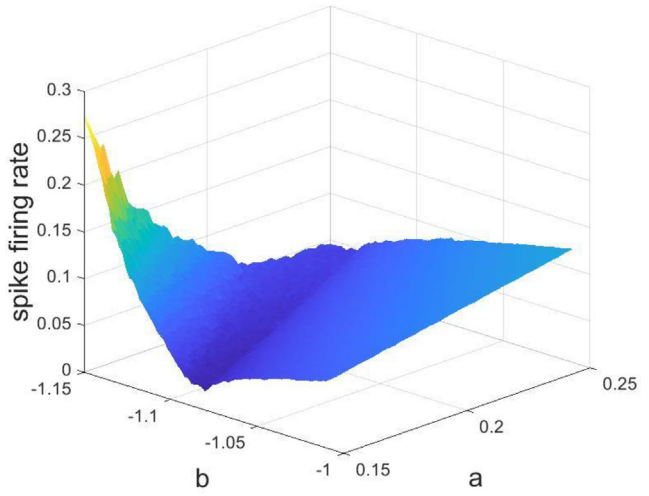

Fig. 6. The spike firing rate of the proposed map by changing a and b. For smaller values of b, increasing a decreases the firing rate. On the other hand, for larger values of b, increasing a increases the spike firing rate.

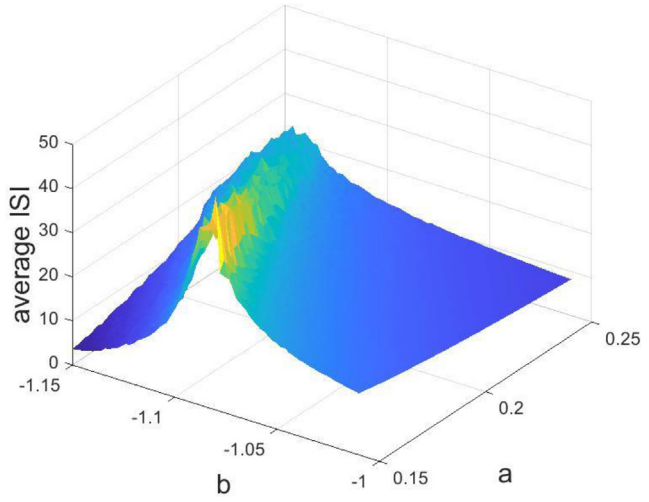

Fig. 7. The average of ISIs for the time series of the map by changing a and b. The average ISI has its largest value, where a has its smallest values, and the b value is -1.08. Compared to Fig. 5, an inverse relationship can be seen among values of the ISI average and the spike firing rate.

starts to increase just after its resetting. However, in experimental data, between two spikes, the voltage has some fluctuation in its rest state (Khaliq et al., 2003). The introduced model can represent these fluctuations. Spike's firing rate is an essential measure for neuronal spiking signals. This measure has been used for studying brain recorded signals (Rolls and Treves, 2011; Gibson et al., 2012). Also, ISI has been used for analyzing neuronal models repetitively in the literature (Zandi-Mehran et al., 2020; Sausedo-Solorio and Pisarchik, 2017). The introduced model could generate time series with a wide range of spiking firing rates, ISI, and complexity.

5. Conclusion

In this paper, a simple 1-dimensional map was introduced to represent the neurons' spiking. The map was designed inspired by the recorded data of a neuron's spikes. Considering the fluctuations of the neurons in their rest state, this model was designed to represent these fluctuations. The map equation was a line that its module (1) was calculated for each iteration. Module (1) function was used for breaking the line curve into two separate pieces. The advantage of using module (1) was a smaller number of equations than other piecewise models of neurons. The piece of the model in the neighborhood of E (1) has generated the rest state fluctuations. The bifurcation diagrams of the system were studied. Also, the value of sample entropy, the firing rate of spikes, and its average were discussed. Considering the simplicity of the introduced map, it can help to model the neuronal collective behaviors in the networks. In other words, a holistic neural model was proposed that can show various dynamics of spiking neurons with wide ranges of firing rates and complexities. Although the a and b parameters did not have a physiological meaning, they had a significant effect on the dynamics of the spiking neurons, which was studied using different measures in this paper.

CRediT authorship contribution statement

Alireza Bahramian: Conceptualization, Software, Writing – original draft. **Janarthanan Ramadoss:** Conceptualization, Validation, Writing – original draft. **Fahimeh Nazarimehr:** Methodology, Validation, Writing – review & editing. **Karthikeyan Rajagopal:** Software, Writing – original draft, Funding acquisition. **Sajad Jafari:** Formal analysis, Writing – review & editing, Supervision. **Iqtadar Hussain:** Investigation, Writing – review & editing, Supervision.

Declaration of Competing Interest

The authors declare that they have no known competing financial interests or personal relationships that could have appeared to influence the work reported in this paper.

Acknowledgment

This work is funded by the Center for Nonlinear Systems, Chennai Institute of Technology, India, vide funding number CIT/CNS/2021/RP-015.

References

AbdelAty, A., Fouda, M.E., Eltawil, A., 2022. On numerical approximations of fractional-order spiking neuron models. Commun. Nonlinear Sci. Numer. Simul. 105, 106078.
Arcas, B.A.Y., Fairhall, A.L., Bialek, W., 2003. Computation in a single neuron: Hodgkin and Huxley revisited. Neural Comput. 15, 1715–1749.
Badel, L., Lefort, S., Berger, T.K., Petersen, C.C.H., Gerstner, W., Richardson, M.J.E., 2008. Extracting non-linear integrate-and-fire models from experimental data using dynamic I-V curves. Biol. Cybern. 99 (4-5), 361–370.
Baer, S.M., Chang, S., Crook, S.M., Gardner, C.L., Jones, J.R., Ringhofer, C., et al., 2021. A multiscale continuum model of the vertebrate outer retina: The temporal dynamics of background-induced flicker enhancement. J. Theor. Biol. 525, 110763.
Bahramian, A., Nouri, A., Baghdadi, G., Gharibzadeh, S., Towhidkhah, F., Jafari, S., 2019. Introducing a chaotic map with a wide range of long-term memory as a model of patch-clamped ion channels current time series. Chaos, Solitons Fractals 126, 361–368.
Bao, H., Chen, C., Hu, Y., Chen, M., Bao, B., 2020. Two-Dimensional Piecewise-Linear Neuron Model. IEEE Transactions on Circuits Systems II: Express Briefs.
Bao, H., Hu, A., Liu, W., Bao, B., 2020. Hidden bursting firings and bifurcation mechanisms in memristive neuron model with threshold electromagnetic induction. IEEE transactions on neural networks learning systems 31 (2), 502–511.
Bao, H., Zhang, Y., Liu, W., Bao, B., 2020. Memristor synapse-coupled memristive neuron network: synchronization transition and occurrence of chimera. Nonlinear Dyn. 100 (1), 937–950.
Bao, B., Zhu, Y., Li, C., Bao, H., Xu, Q., 2020. Global multistability and analog circuit implementation of an adapting synapse-based neuron model. Nonlinear Dyn. 101, 1105–1118.
Batista, A.M., Pinto, S.E.d.S., Viana, R.L., Lopes, S.R., 2002. Lyapunov spectrum and synchronization of piecewise linear map lattices with power-law coupling. Phys. Rev. E 65, 056209.

Bhalla, U.S., 2012. In: Computational Systems Neurobiology. Springer Netherlands, Dordrecht, pp. 193–225. https://doi.org/10.1007/978-94-007-3858-4_7.
Brette, R., Pillow, J.W., 2015. What is the most realistic single-compartment model of spike initiation? PLoS Comput Biol 11 (4), e1004114.
Bush, P.C., Sejnowski, T.J., 1993. Reduced compartmental models of neocortical pyramidal cells. J. Neurosci. Methods 46 (2), 159–166.
Cazelles, B., Courbage, M., Rabinovich, M., 2001. Anti-phase regularization of coupled chaotic maps modelling bursting neurons. EPL 56 (4), 504–509.
Channell Jr, P., Cymbalyuk, G., Shilnikov, A., 2007. Applications of the poincare mapping technique to analysis of neuronal dynamics. Neurocomputing 70, 2107–2111.
Churchland, M.M., Shenoy, K.V., 2007. Temporal complexity and heterogeneity of single-neuron activity in premotor and motor cortex. J. Neurophysiol. 97, 4235–4257.
Courbage, M., Nekorkin, V.I., 2010. Map based models in neurodynamics. International Journal of Bifurcation Chaos 20, 1631–1651.
Destexhe, A., Rudolph, M., Fellous, J.-M., Sejnowski, T.J., 2001. Fluctuating synaptic conductances recreate in vivo-like activity in neocortical neurons. Neuroscience 107 (1), 13–24.
Dong, Y., Liang, Y., Wang, G., Iu, H.-C., 2021. Chua Corsage memristor based neuron models. Electron. Lett. 57 (24), 903–905.
Doya, K., Selverston, A.I., 1994. Dimension reduction of biological neuron models by artificial neural networks. Neural Comput. 6 (4), 696–717.
FitzHugh, R., 1955. Mathematical models of threshold phenomena in the nerve membrane. The bulletin of mathematical biophysics 17 (4), 257–278.
FitzHugh, R., 1961. Impulses and physiological states in theoretical models of nerve membrane. Biophys. J . 1 (6), 445–466.
Ge, M., Jia, Y.a., Kirunda, J.B., Xu, Y., Shen, J., Lu, L., Liu, Y., Pei, Q., Zhan, X., Yang, L., 2018. Propagation of firing rate by synchronization in a feed-forward multilayer Hindmarsh-Rose neural network. Neurocomputing 320, 60–68.
Gentili, P.L., Bartolomei, B., Micheau, J.-C., 2021. Light-driven artificial neuron models based on photoswitchable systems. Dyes Pigm. 187, 109086.
Gibson, S., Judy, J.W., Markovic, D., 2012. Spike sorting: The first step in decoding the brain: The first step in decoding the brain. IEEE Signal Process Mag. 29 (1), 124–143.
Girardi-Schappo, M., Tragtenberg, M.H.R., Kinouchi, O., 2013. A brief history of excitable map-based neurons and neural networks. J. Neurosci. Methods 220 (2), 116–130.
Guo, Y., Dong, Q., Wang, L., Lou, X., 2020. Dynamical Complexity of FHN Neuron System Driven by Correlated Noises and Periodic Signal. Fluctuation Noise Letters, 2150012.
S. He, "Complexity and Chimera States in a Ring-Coupled Fractional-Order Memristor Neural Network," *Front. Appl. Math. Stat.,* 2020.
Henze, D.A., Borhegyi, Z., Csicsvari, J., Mamiya, A., Harris, K.D., Buzsáki, G., 2000. Intracellular features predicted by extracellular recordings in the hippocampus in vivo. J. Neurophysiol. 84 (1), 390–400.
Herz, A.V.M., Gollisch, T., Machens, C.K., Jaeger, D., 2006. Modeling single-neuron dynamics and computations: a balance of detail and abstraction. Science 314 (5796), 80–85.
Hodgkin, A., Huxley, A., 1990. A quantitative description of membrane current and its application to conduction and excitation in nerve. Bull. Math. Biol. 52 (1-2), 25–71.
Ibarz, B., Cao, H., Sanjuán, M.A., 2008. Bursting regimes in map-based neuron models coupled through fast threshold modulation. Phys. Rev. E 77, 051918.
Ibarz, B., Casado, J.M., Sanjuán, M.A.F., 2011. Map-based models in neuronal dynamics. Phys. Rep. 501 (1-2), 1–74.
Izhikevich, E.M., 2003. Simple model of spiking neurons. IEEE Trans. Neural Networks 14, 1569–1572.
Izhikevich, E.M., 2004. Which model to use for cortical spiking neurons? IEEE Trans. Neural Networks 15, 1063–1070.
Izhikevich, E.M., Hoppensteadt, F., 2004. Classification of bursting mappings. International Journal of Bifurcation Chaos 14, 3847–3854.
Jia, Y., Gu, H., Luo, Q., 2017/08/11 2017.. Sample entropy reveals an age-related reduction in the complexity of dynamic brain. Sci. Rep. 7, 7990.
Kasimova, M.A., Yazici, A., Yudin, Y., Granata, D., Klein, M.L., Rohacs, T., et al., 2018. Ion channel sensing: Are fluctuations the crux of the matter? The journal of physical chemistry letters 9, 1260–1264.
Khaleghi, L., Panahi, S., Chowdhury, S.N., Bogomolov, S., Ghosh, D., Jafari, S., 2019. Chimera states in a ring of map-based neurons. Physica A: Statistical Mechanics its Applications 536, 122596.
Khaliq, Z.M., Gouwens, N.W., Raman, I.M., 2003. The contribution of resurgent sodium current to high-frequency firing in Purkinje neurons: an experimental and modeling study. J. Neurosci. 23, 4899–4912.
Li, K., Bao, H., Li, H., Ma, J., Hua, Z., Bao, B., 2022. Memristive Rulkov Neuron Model with Magnetic Induction Effects. IEEE Trans. Ind. Inf. 18 (3), 1726–1736.
Liu, Y., Ma, J., Xu, Y., Jia, Y., 2019. Electrical Mode Transition of Hybrid Neuronal Model Induced by External Stimulus and Electromagnetic Induction. Int. J. Bifurcation Chaos 29, 1950156.
LoFaro, T., Kopell, N., 1999. Timing regulation in a network reduced from voltage-gated equations to a one-dimensional map. J. Math. Biol. 38 (6), 479–533.
Ma, J., Tang, J., 2015. A review for dynamics of collective behaviors of network of neurons. Science China Technological Sciences 58, 2038–2045.
Ma, J., Tang, J., 2017. A review for dynamics in neuron and neuronal network. Nonlinear Dyn. 89, 1569–1578.
Ma, J., Yang, Z.-Q., Yang, L.-J., Tang, J., 2019. A physical view of computational neurodynamics. J. Zhejiang University-Science A 20 (9), 639–659.
Mainen, Z.F., Sejnowski, T.J., 1996. Influence of dendritic structure on firing pattern in model neocortical neurons. Nature 382 (6589), 363–366.
O. V. Maslennikov and V. I. Nekorkin, "Map-based approach to problems of spiking neural network dynamics," in *Nonlinear dynamics and complexity*, ed: Springer, 2014, pp. 143-161.
Medvedev, G.S., 2005. Reduction of a model of an excitable cell to a one-dimensional map. Physica D 202 (1-2), 37–59.
Mesbah, S., Moghtadaei, M., Hashemi Golpayegani, M.R., Towhidkhah, F., 2014. One-dimensional map-based neuron model: A logistic modification. Chaos, Solitons Fractals 65, 20–29.
Morris, C., Lecar, H., 1981. Voltage oscillations in the barnacle giant muscle fiber. Biophys. J . 35 (1), 193–213.
Nagumo, J., Arimoto, S., Yoshizawa, S., 1962. An active pulse transmission line simulating nerve axon. Proc. IRE 50, 2061–2070.
Naundorf, B., Wolf, F., Volgushev, M., 2006. Unique features of action potential initiation in cortical neurons. Nature 440, 1060–1063.
Obeid, I., Wolf, P.D., 2004. Evaluation of spike-detection algorithms fora brain-machine interface application. IEEE Trans. Biomed. Eng. 51 (6), 905–911.
Palmieri, I., Monteiro, L.H.A., Miranda, M.D., 2015. The transfer function of neuron spike. Neural Networks 68, 89–95.
Pasemann, F., 1997. A simple chaotic neuron. Physica D 104 (2), 205–211.
Pietras, B., Gallice, N., Schwalger, T., 2020. Low-dimensional firing-rate dynamics for populations of renewal-type spiking neurons. Phys. Rev. E 102, 022407.
Richman, J.S., Moorman, J.R., 2000. Physiological time-series analysis using approximate entropy and sample entropy. American Journal of Physiology-Heart Circulatory Physiology 278, 2039–2049.
Rolls, E.T., Treves, A., 2011. The neuronal encoding of information in the brain. Prog. Neurobiol. 95 (3), 448–490.
Rotstein, H.G., Oppermann, T., White, J.A., Kopell, N., 2006. A reduced model for medial entorhinal cortex stellate cells: subthreshold oscillations, spiking and synchronization. J. Comput. Neurosci. 21, 271–292.
Rouhani, M., Baer, S.M., Crook, S.M., 2021. A stage-structured population model for activity-dependent dendritic spines. J. Biol. Dyn. 15 (sup1), S62–S80.
Rulkov, N.F., 2002. Modeling of spiking-bursting neural behavior using two-dimensional map. Phys. Rev. E 65, 041922.
N. F. Rulkov, I. Timofeev, and M. Bazhenov, "Oscillations in large-scale cortical networks: map-based model," *Journal of computational neuroscience,* vol. 17, pp. 203-223, 2004.
Sanchez, P.J., 2006. As simple as possible, but no simpler: a gentle introduction to simulation modeling. In: Proceedings of the 2006 winter simulation conference, pp. 2–10.
Sausedo-Solorio, J., Pisarchik, A., 2017. Synchronization in network motifs of delay-coupled map-based neurons. The European Physical Journal Special Topics 226, 1911–1920.
Schwalger, T., Chizhov, A.V., 2019. Mind the last spike—firing rate models for mesoscopic populations of spiking neurons. Curr. Opin. Neurobiol. 58, 155–166.
Wang, S., He, S., Rajagopal, K., Karthikeyan, A., Sun, K., 2020. Route to hyperchaos and chimera states in a network of modified Hindmarsh-Rose neuron model with electromagnetic flux and external excitation. The European Physical Journal Special Topics 229 (6-7), 929–942.
Wang, C., Ma, J., 2018. A review and guidance for pattern selection in spatiotemporal system. Int. J. Mod Phys B 32, 1830003.
Wilson, H.R., Cowan, J.D., 1972. Excitatory and inhibitory interactions in localized populations of model neurons. Biophys. J . 12 (1), 1–24.
Wolf, A., Swift, J.B., Swinney, H.L., Vastano, J.A., 1985. Determining Lyapunov exponents from a time series. Physica D 16 (3), 285–317.
Wu, F., Ma, J., Zhang, G.e., 2019. A new neuron model under electromagnetic field. Appl. Math. Comput. 347, 590–599.
Zandi-Mehran, N., Panahi, S., Hosseini, Z., Golpayegani, S.M.R.H., Jafari, S., 2020. One dimensional map-based neuron model: A phase space interpretation. Chaos, Solitons Fractals 132, 109558.
Zhang, D., Ding, H., Liu, Y., Zhou, C., Ding, H., Ye, D., 2009. Neurodevelopment in newborns: a sample entropy analysis of electroencephalogram. Physiol. Meas. 30 (5), 491–504.
Zhang, S., Zheng, J., Wang, X., Zeng, Z., He, S., 2020. Initial offset boosting coexisting attractors in memristive multi-double-scroll Hopfield neural network. Nonlinear Dyn. 102, 2821–2841.